

# Liquid crystallinity in flexible and rigid rod polymers

Galen T. Pickett

*Department of Physics and Astronomy, California State University, Long Beach,  
1250 Bellflower Boulevard, Long Beach, California 90840*

Kenneth S. Schweizer

*Departments of Materials Science and Engineering and Chemistry, and Materials Research Laboratory,  
University of Illinois, 1304 West Green Street, Urbana, Illinois 61801*

(Received 2 August 1999; accepted 17 December 1999)

We apply an anisotropic version of the polymer reference interaction site model (PRISM) integral equation description of flexible polymers to analyze athermal liquid crystallinity. The polymers are characterized by a statistical segment length,  $\sigma_o$ , and by a physical hard-core thickness,  $d$ , that prevents the overlap of monomers on different chains. At small segment densities,  $\rho$ , the microscopic length scale  $d$  is irrelevant (as it must be in the universal semidilute regime), but becomes important in concentrated solutions and melts. Under the influence of the excluded volume interactions alone, the chains undergo a lyotropic, first-order isotropic–nematic transition at a concentration dependent upon the dimensionless “aspect ratio,”  $\sigma_o/d$ . The transition becomes weaker as  $d \rightarrow 0$ , becoming second order, as has been previously shown. We extend the theory to describe the transition of rigid, thin rods, and discuss the evolution of the anisotropic liquid structure in the ordered phase. © 2000 American Institute of Physics. [S0021-9606(00)51510-4]

## I. INTRODUCTION

If studying anisotropy in liquids is a goal, then surely the most important and compelling phenomenon for investigation is liquid crystallinity.<sup>1–3</sup> The unique, and highly useful, properties of liquid crystalline materials derive in whole from the partial ordering of their microscopic degrees of freedom. An important subclass of such materials is liquid crystalline polymers (LCP's) which have many design advantages. The extended nature of polymers, and consequently their ability to interpenetrate and entwine, gives polymer solutions generally, and LCP solutions in particular, a very interesting “universal” behavior in semidilute solution.<sup>4–6</sup> This concentration regime is characterized by a low absolute polymer concentration (typically  $\leq 20\%$ ) yet maintains highly correlated collective properties. As we have recently shown, the semidilute regime of even ordinary flexible polymers has the possibility of undergoing, at least in a mean field sense, a continuous transition to homogeneous, yet anisotropic, states.<sup>7</sup>

The synthesis and control of LCP's is facilitated by two general design strategies, or classes, of liquid crystalline polymers. Side chain polymers have rigid, rodlike mesogens bonded to a flexible backbone polymer, and the liquid crystalline transition is usually induced by lowering the temperature of a dense, neat sample (thermotropic transition). Main-chain LCP's on the other hand, have monomers made entirely of stiff rodlike mesogens, or have the mesogens separated by flexible spacers. Moreover, even nominally “flexible chains” with aspect ratios of order unity such as polyethylene, polyphosphazines and polydiethylsiloxane, have all been reported to exhibit liquid crystalline behavior in the melt under ambient and/or high pressure conditions.<sup>8</sup>

The polymer reference interaction site model (PRISM)<sup>9</sup>

is known to give an accurate description of structure and thermodynamics in homogeneous, isotropic polymer solutions, melts and blends. Recently, the range of PRISM has been extended to include *anisotropic* chain conformations.<sup>7,10</sup> While we will not pursue an atomistically detailed theory based on a particular mesogen/backbone combination, the theory clearly has the potential to encompass such a calculation. In this initial work we pursue an approximate theory that provides a rough description of any single component LCP characterized by two competing length scales. The first is the statistical length scale,  $\sigma_o$ ,<sup>4,5</sup> which characterizes the relative local stiffness of the polymer backbone. The second is the monomer effective hard-core diameter,  $d$ , the physical *thickness* of the chain. For typical flexible polymers,  $\sigma_o \approx d$ , so that the chain can be envisioned as a set of tangent-connected spherical sites. On the other hand, typical (but not all) thermotropic LCP's have  $\sigma_o \approx 5d$  and greater, corresponding to quite a high aspect ratio. We shall ignore all other chemical details. In this paper, we specialize solely to *athermal* excluded volume interactions between monomer sites. Thus, the transition we exhibit below is most properly thought of as a *lyotropic* transition, where the increasing concentration of polymer triggers the phase transition.

We focus on the isotropic-to-nematic (I–N) transition for our model LCP's. This is the simplest liquid crystalline transition to study, as it is characterized by the development of *orientational* order on a single axis, while all other degrees of freedom are liquidlike.<sup>2</sup> It is perhaps possible to go beyond the nematic phase and describe phases with translational modulations (such as the smectic) either directly within an integral equation formalism, or by combining anisotropic PRISM theory with a density functional theory (DFT)<sup>9,11</sup> approach.

The fundamental ideas behind anisotropic PRISM were developed in the preceding paper.<sup>10</sup> For economy of expression, we assume the reader is familiar with that work (hereafter referred to as Paper I). All symbols and notation in the present paper are consistent with Paper I, and we shall quote equations as Eq. (I.xx). In this work, we construct an anisotropy-dependent free energy whose minimization will control the I–N transition. We first discuss this transition in one universal ( $d \rightarrow 0$ ) limit (so-called “thread”<sup>7,12</sup> model) and then treat the finite  $d$  transition. In addition to the thermodynamics of the athermal I–N phase diagram, we also characterize the fluid structure through the transition, demonstrating an anisotropic behavior of the contact value of the pair correlation (relevant for a discussion of self-diffusion and dynamics<sup>13</sup>), and the anisotropic screening of density fluctuations. Finally, to provide a benchmark to evaluate this theory, we work out its predictions for a simple model of the Onsager transition of long, thin, rigid rods.<sup>3</sup> Overall, the transition our theory predicts is weaker than is observed experimentally, or in the exact calculation of Onsager. We also discuss the role of weak attractive forces.

## II. ANISOTROPIC PRISM: THEORY AND CHAIN MODEL

We take as our starting point the chain model of Paper I. That is, the polymer chains are anisotropic random walks

$$\omega(\mathbf{q}) = \frac{N}{1 + (N\sigma_{\perp}^2 q_{\perp}^2/4) + (N\sigma_z^2 q_z^2/4)}, \quad (1)$$

where  $\sigma_z = \sigma_o(1 + 2\tau)^{1/2}3^{-1/2}$ , and  $\sigma_{\perp} = \sigma_o(1 + \tau)^{1/2}3^{-1/2}$ , consistent with Eq. (I.21–I.23). Thus,  $\tau$  is the standard nematic order parameter describing the orientation of *statistical segment scale* lengths of chain.  $\omega(\mathbf{q})$  describes aligned, but not stretched chains, in that  $6R_g^2 = N(\sigma_{\perp}^2 + \sigma_{\perp}^2 + \sigma_z^2)$  is independent of  $\tau$ .<sup>14</sup> Our approach can be extended “self-consistently” to allow for chain deformations which modify  $R_g$  in response to intermolecular forces, but we shall not pursue this more complicated generalization here.<sup>15</sup>

The collective structure factor,  $S(\mathbf{q})$ , is given by

$$S(\mathbf{q}) = \frac{S_o}{1 + \xi_{\perp}^2 q_{\perp}^2 + \xi_z^2 q_z^2}, \quad (2)$$

where the dimensionless inverse compressibility is  $S(\mathbf{q}=0) \equiv S_o = kT\rho\kappa_T$  and the *anisotropic* density screening lengths are

$$\xi_z = \frac{\sigma_z}{2} \sqrt{S_o}, \quad (3)$$

$$\xi_{\perp} = \frac{\sigma_{\perp}}{2} \sqrt{S_o}. \quad (4)$$

Here,  $\kappa_T$  is the isothermal compressibility, and we set Boltzmann’s constant multiplied by temperature  $kT=1$  below. Density fluctuations are correlated differently along the nematic director than perpendicular to it, as long as  $\tau \neq 0$ .

We shall consider three separate, though related, closures; namely, the thread, string, and cutoff thread models. They are all “one parameter” closures that leave the direct

correlation function unspecified up to a multiplicative constant. Both the string and the cutoff thread models introduce the physical thickness of the chains,  $d$ , in approximate ways. The thread model is recovered when  $d \rightarrow 0$ . Since  $d$  is the only chemical length scale for our model polymers, it is not surprising that the thread model correctly captures the *universal* regime of semidilute densities, where all chemical details become irrelevant.<sup>4,16</sup> The string closure accounts for a nonzero value for  $d$  by *demanding* that  $g(r)$  vanish on average for  $r < d$ , so that  $g(\mathbf{r}) < 0$  near  $r=0$ . The “physical region” of the theory is  $r > d$ , for which the pair correlation is always positive in the isotropic phase.<sup>12</sup> This condition breaks down drastically when we consider *anisotropic* phases below. A remedy for the negativity of  $g(\mathbf{r})$  is the “cutoff thread” closure of Paper I:<sup>10</sup>

$$C(\mathbf{q}) = c_o, \quad \text{when } q < \frac{\pi b}{d} \\ = 0, \quad \text{otherwise,} \quad (5)$$

along with the pointwise core condition,  $g(\mathbf{r}) \equiv 0$ . Here,  $b$  is a numerical constant of order unity which links the true hard-core diameter with an ultraviolet wavevector cutoff for  $C(\mathbf{q})$ . This is the closure we shall employ to investigate liquid crystallinity for athermal polymers, outside the universal regime,  $d \rightarrow 0$ , or  $\rho \rightarrow 0$ . Notice that direct correlations are no longer propagated at contact, but rather over a range roughly of  $r \approx d/b$ .

Chain stiffness is modeled by choosing the “aspect ratio”  $\sigma_o/d > 1$ . Explicit chain rigidity is *not* included in this work, but a suitable choice of  $\omega(\mathbf{q})$ <sup>9,17</sup> will allow a more realistic treatment of liquid crystallinity of semiflexible polymers. We expect our present simple treatment will underestimate the orienting ability of chains, and this has significant consequences for the phase behavior predicted.

As pointed out in Paper I, the cutoff model closure is analytically executable in two limits: the small density “semidilute” regime, and in the maximum density state for which  $S(\mathbf{q})=0$  for all  $\mathbf{q}$ . Interpolating between these limits yields an analytic expression for  $S_o$

$$S_o^{-1} = \frac{4}{3} \left| \frac{\rho' b \sigma_o}{d} \right|^2 (1 - \tau)^2 (1 + 2\tau) \left( 1 - \frac{\rho'}{\rho'_{\max}} \right)^{-1}, \quad (6)$$

where  $S_o$  vanishes when  $\rho' = \rho'_{\max}$

$$\rho'_{\max} = \frac{2b\sqrt{3} \tan^{-1} \sqrt{3\tau/(1-\tau)}}{\pi d \sigma_o^2 \sqrt{\tau(1-\tau)}}. \quad (7)$$

The scaled density  $\rho'$  is defined to be

$$\rho' = \frac{\pi}{6} \rho \sigma_o^2 d, \quad (8)$$

and equals 1 for the isotropic phase incompressible state. For  $\tau \neq 0$ ,  $\rho'_{\max} > 1$ , so, as expected physically, the liquid crystalline phases are capable of being packed more efficiently than isotropically oriented chains. Unfortunately,  $\rho'_{\max} \rightarrow \infty$  as  $\tau \rightarrow 1$  in the present model. In reality, we can expect the maximum density of the nematic phase to exceed that of the isotropic phase by perhaps as much as 30%. To mimic this

physically reasonable behavior, for the purposes of discussion and presentation of plots we shall take  $\rho' = 1$  as the maximal density attainable for *all*  $\tau$ , although predictions for  $\rho' > 1$  are available.

Interestingly, with the redefinition

$$\rho'_{\text{string}} = \rho \frac{9d_{\text{string}}\sigma_o^2}{2\pi}, \quad (9)$$

the interpolated closure from the string model implies that the string model inverse compressibility is also given by Eq. (6). There is an inherent ambiguity in the choice of  $d/b$  in the cutoff model that is not apparent in the string model. Namely, the length scale at which it is appropriate to cut  $C(\mathbf{q})$  off clearly must scale as  $d$ , but the prefactor is unspecified. If we let

$$d_{\text{cutoff}} = \frac{4}{3}d_{\text{string}}, \quad (10)$$

that is,  $b = 4/3$ , then the interpolated closures for the models agree exactly, and the  $S_o$  from each model is given by Eq. (6). Since the string model can be justified as an optimized perturbation treatment around a thread reference,<sup>12</sup> it is reassuring that the two models agree when  $b$  is numerically close to 1. In what follows, we take  $b = 1$ . Merely rescaling  $d$  in the results below will allow a different choice of  $b$ .

### III. FREE ENERGY PER SITE

Our primary goal is to construct a free energy function for  $\tau$  which, when minimized, gives a prescription for determining the *equilibrium* value of  $\tau$ . The fact that experimentally the initially observed liquid crystalline transitions are universally from the isotropic to the nematic ( $\tau > 0$ ) certainly leads one to believe that such a free energy should predict a discontinuous jump in  $\tau$  to positive values near the transition, as we indeed find below.

In the  $\rho'$ , temperature *and*  $\tau$  ensemble (that is, we hold all three quantities fixed), this is easily accomplished through standard thermodynamic relations

$$S_o^{-1} = \left. \frac{\partial P}{\partial \rho} \right|_{T, \tau} \rightarrow P = \int_0^\rho dx S_o^{-1}(x; \tau), \quad (11)$$

$$F_{\text{site}} = \int_0^\rho \frac{dx}{x^2} P(x; \tau). \quad (12)$$

Here,  $P$  is the pressure, and  $F_{\text{site}}$  is the many-chain contribution to the per-site free energy. The detailed  $\rho'$  and  $\tau$  dependence of  $F_{\text{site}}$  is

$$F_{\text{site}} = \frac{2\sigma_o^2(1-\tau)^2(1+2\tau)\rho'_{\text{max}}}{3d^2\rho'} \left( \rho'(2\rho'_{\text{max}} - \rho') + 2(\rho'_{\text{max}} - \rho') \log \left[ 1 - \frac{\rho'}{\rho'_{\text{max}}} \right] \right). \quad (13)$$

This ‘‘compressibility’’ route to the free energy is the most appropriate given the fact that thread PRISM-PY (Percus–Yevick) theory is equivalent to a self-consistent Gaussian field theory for constrained collective density fluctuations.<sup>18</sup> The prefactor in  $F_{\text{site}}$  indicates that as  $\tau$  becomes nonzero,

$F_{\text{site}}$  is lowered since alignment causes each chain to occupy a smaller spanned volume, overlapping less with its neighbors. This results in a smaller repulsive excess free energy. As in the original Onsager treatment of the I–N transition, it is this many body term (limited to the second virial term in the Onsager theory) which drives the transition toward  $|\tau| > 0$ .

$F_{\text{site}}[\tau]$  is not the entire free energy for chains held at a constant  $\tau$ . We must address the entropy cost per site to maintain the chains in an anisotropic distribution of orientations. For Gaussian Markov chains, the question can be answered on a per-site basis. The partition function for a single anisotropic Gaussian chain is<sup>6</sup>

$$\begin{aligned} Z[\sigma_z, \sigma_\perp] &= \left[ \int dx dy dz \exp \left[ \frac{-3x^2}{2\sigma_\perp^2} \right] \right. \\ &\quad \times \left. \exp \left[ \frac{-3y^2}{2\sigma_\perp^2} \right] \exp \left[ \frac{-3z^2}{2\sigma_z^2} \right] \right]^N \\ &= \left[ \frac{2\pi}{3} \right]^{3N/2} \sigma_\perp^{2N} \sigma_z^N. \end{aligned} \quad (14)$$

Thus, in the isotropic case<sup>4,6</sup>

$$Z_o \equiv \left[ \int d^3r \exp \left[ -\frac{r^2}{\sigma_o^2} \right] \right]^N = \left[ \frac{2\pi}{3} \right]^{3N/2} \sigma_o^{3N}. \quad (15)$$

The entropy cost required to maintain  $\sigma_\perp \neq \sigma_z \neq \sigma_o$  for a single site is thus

$$F_{\text{ideal}} = -\frac{1}{N} \log[Z/Z_o] = -\log \frac{\sigma_\perp^2 \sigma_z}{\sigma_o^3}. \quad (16)$$

In terms of the nematic order parameter,  $\tau$ , we have:

$$F_{\text{ideal}}[\tau] = -\log[(1-\tau)\sqrt{1+2\tau}]. \quad (17)$$

It clearly works towards stabilizing the isotropic phase.

The total free energy per site for chains held at a particular homogeneous  $\rho'$ , and a fixed order parameter is

$$F_{\text{tot}}[\tau] = F_{\text{site}}[\tau] + F_{\text{ideal}}[\tau]. \quad (18)$$

We can pass from the constant- $\tau$  ensemble to the true equilibrium situation by determining which of all the possible  $\tau$  minimizes the free energy. Thus,  $\tau_{\text{eq}}$  is given by

$$\left. \frac{\partial F_{\text{tot}}[\tau]}{\partial \tau} \right|_{\tau = \tau_{\text{eq}}(\rho')} \equiv 0. \quad (19)$$

Figure 1 shows how this minimization plays out with  $d = \sigma_o/2$ . If  $\rho' < \rho_c = 0.8753$ , the isotropic solution minimizes  $F_{\text{tot}}$ . Beyond  $\rho_c$ , however, the nematic solution becomes most stable. A metastable  $\tau < 0$  discotic solution appears, as well. To show that this is the case generally, it suffices to investigate the small- $\tau$  behavior of  $F_{\text{tot}}$

$$F_{\text{tot}} = F_0 + F_2 \tau^2 + F_3 \tau^3 + O[\tau^4]. \quad (20)$$

The relevant expansion coefficients are

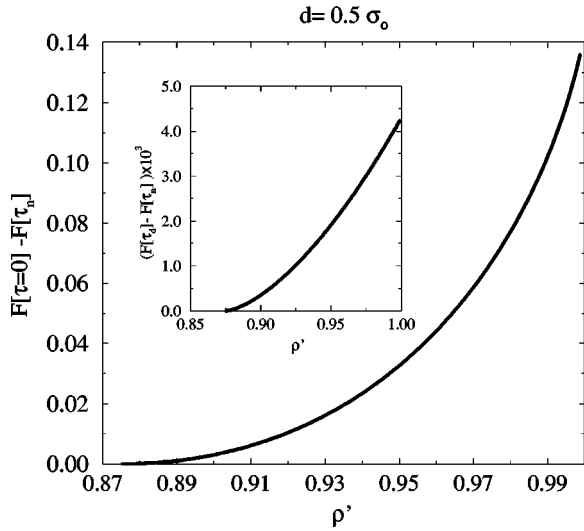


FIG. 1. Relative stability of I, N, D phases when  $\sigma_o = 2d$ . The nematic phase overtakes the stability of the isotropic phase, when  $\rho' = 0.8753$ . Inset is the amount by which the nematic phase is stable relative to the *discotic* phase.

$$F_2 = \frac{3}{2} + \frac{2\sigma_o^2}{15d^2}(11\rho' - 6) + \frac{4\sigma_o^2}{15d^2\rho'}(7\rho' - 3)\log(1 - \rho'), \quad (21)$$

$$F_3 = -1 - \frac{4\sigma_o^2}{105d^2}(27\rho' - 22) - \frac{8\sigma_o^2}{105d^2\rho'}(19\rho' - 11)\log(1 - \rho'). \quad (22)$$

The isotropic solution to Eq. (19) becomes linearly unstable in  $\tau$  when  $F_2$  goes from positive to negative, at

$$\frac{d^2}{\sigma_o^2} = \frac{4}{45}(6 - 11\rho') + \frac{8}{45\rho'}(3 - 7\rho')\log(1 - \rho'). \quad (23)$$

If we evaluate  $F_3$  under the condition given by Eq. (23), one can infer the linear stability of the nematic phase, just at its incipient arrival<sup>2,6</sup>

$$F_3 = \frac{4\rho'(\rho' - 6) + (4\rho' - 6)\log(1 - \rho')}{7\rho'(11\rho' - 6) + 2(7\rho' - 3)\log(1 - \rho')}. \quad (24)$$

$F_3$  is always *negative* when Eq. (23) holds, so  $F_{\text{tot}}$  behaves as

$$\frac{F_{\text{tot}}}{F_0} = 1 - |c_3|\tau^3 + |c_4|\tau^4 + \dots, \quad (25)$$

where  $c_3$  and  $c_4$  are nonzero. The free energy decreases initially as  $\tau$  becomes positive. Thus, we can be assured that  $\tau_{\text{eq}} > 0$  near the transition, and Fig. 1 indicates that this trend is continued far into the ordered phase. Thus, the theory always predicts a first-order I–N transition.<sup>2,6</sup> As we see below, however, the discontinuity in  $\tau$  at the transition is exceedingly small.

#### IV. THREAD MODEL TRANSITION

Before we consider the detailed predictions based on Eq. (18) for arbitrary  $d$ , it is helpful for a basis of comparison to consider first  $d \rightarrow 0$ , the so-called thread limit.<sup>7,12</sup> Here, we consider only the limiting  $N \rightarrow \infty$  case, although the general finite  $N$  situation is also easily worked out as discussed previously.<sup>7,10</sup> Equation (8) indicates that taking  $d \rightarrow 0$  is equivalent to a small  $\rho'$  expansion. Taking the  $\rho'$  expansion of Eq. (18) up to second order, and rewriting the expression in terms of  $\rho$  yields:

$$F_{\text{tot}}^{\text{thread}}[\rho, \tau] = \frac{\pi^2}{648} \rho^2 \sigma_o^6 (1 - \tau)^2 (1 + 2\tau) - \log[(1 - \tau)\sqrt{1 + 2\tau}]. \quad (26)$$

The equation of state for fixed  $\tau$  is

$$P^{\text{thread}} = \frac{\pi^2}{324} \rho^3 \sigma_o^6 (1 - \tau)^2 (1 + 2\tau). \quad (27)$$

The equation of state is a *power-law* in  $\rho$ , the total site density. The  $P \sim (\rho\sigma_o^2)^3$  law (with a  $\tau$ -dependent prefactor) is appropriate for the universal semidilute behavior of polymer solutions.<sup>4,6</sup> The dimensionless, constant- $\tau$ , isothermal compressibility is

$$S_o^{\text{thread}} = \left[ \frac{4}{3} \left| \frac{\rho' \sigma_o}{d} \right|^2 (1 - \tau)^2 (1 + 2\tau) \right]^{-1}. \quad (28)$$

The latter expression determines the spectrum of collective density fluctuations *while  $\tau$  is held fixed*. When we allow  $\tau \rightarrow \tau_{\text{eq}}(\rho)$  in response to minimizing  $F_{\text{tot}}^{\text{thread}}$ , a different expression holds which captures the fact that as  $\rho$  fluctuates, so too does  $\tau_{\text{eq}}(\rho)$ .

It is interesting that  $\tau$  enters Eq. (26) in the combination  $(1 - \tau)\sqrt{1 + 2\tau}$ . Physically, this is the *invaded volume* of a single site, compared to that of an isotropically oriented site

$$(1 - \tau)\sqrt{1 + 2\tau} \sim \frac{\sigma_{\perp}^2 \sigma_z}{\sigma_o^3}. \quad (29)$$

The minimization of  $F_{\text{tot}}^{\text{thread}}$ , therefore, determines the quantity  $\sigma_{\perp}^2 \sigma_z$

$$(1 - \tau_{\text{eq}})\sqrt{1 + 2\tau_{\text{eq}}} = \frac{\rho}{\rho_c}. \quad (30)$$

Remarkably, when  $\rho > \rho_c = 18/(\pi\sigma_o^3)$ , there are *two* nonzero values of  $\tau$  that minimize  $F_{\text{tot}}^{\text{thread}}$ , one positive and one negative. Degenerate nematic and discotic ordered phases coexist. We verify that the transition is *continuous* by inspecting the  $\tau$  expansion

$$F_{\text{tot}}^{\text{thread}} = \frac{\pi^2 \sigma_o^6 \rho^2}{648} + \frac{3}{2} \left( 1 - \frac{\rho^2}{\rho_c^2} \right) \tau^2 - \left( 1 - \frac{\rho^2}{\rho_c^2} \right) \tau^3 + \frac{9}{4} \tau^4 + O[\tau^5]. \quad (31)$$

As long as  $\rho < \rho_c$ ,  $F_{\text{tot}}^{\text{thread}}$  displays a single minima at  $\tau = 0$ . At  $\rho = \rho_c$ , we see that the coefficient of the  $\tau^2$  and the coefficient of the  $\tau^3$  term simultaneously vanish. Symmetry

conditions normally require the  $O[\tau^3]$  term to be nonzero near the I–N transition,<sup>2</sup> because  $\tau > 0$  and  $\tau < 0$  are quite different physical situations. There is no obvious physical symmetry for ordinary liquid crystals which removes the  $\tau^3$  term at the transition. However, for thread polymers, there is a symmetry allowing (indeed, requiring) us to link every single nematic ( $\tau > 0$ ) solution uniquely to a particular discotic ( $\tau < 0$ ) solution, through Eq. (30).

We can easily determine the equation of state for the thread chains with  $\tau = \tau_{\text{eq}}(\rho')$ <sup>7</sup>

$$P_{\text{eq}}^{\text{thread}} = \frac{18}{\pi\sigma_o^3} \left| \frac{\rho}{\rho_c} \right|^3 = \frac{\pi^2 \rho^3 \sigma_o^6}{324} \quad \text{when } \rho < \rho_c, \quad (32)$$

$$= \frac{18}{\pi\sigma_o^3} \frac{\rho}{\rho_c} = \rho \quad \text{when } \rho > \rho_c. \quad (33)$$

Thus, liquid crystal threads behave as an ideal-gas of *disconnected* segments, at least with regards to the equation of state, in the ordered phase. The ordered liquid is, however, far from an ideal gas. It is a highly correlated, anisotropic fluid with a long-range (although anisotropic) correlation hole in  $g(\mathbf{r})$ . The transition is continuous and therefore the pressure can be inverted into a single-valued function giving the density of the system as a function of applied pressure. This is no longer the case when a finite  $d$  appears in the model. With an extra length scale beyond  $\sigma_o$ ,  $F_{\text{tot}}$  is no longer a simple function of  $\rho\sigma_{\perp}^2\sigma_z$ , as  $F_{\text{tot}}^{\text{thread}}$  is, and we see below this drives the discotic solution to metastability, and makes the transition discontinuous.

The *equilibrium* inverse compressibility can be defined as

$$(\rho\kappa)^{-1} \equiv \left. \frac{\partial P_{\text{eq}}^{\text{thread}}}{\partial \rho} \right|_T = 1, \quad (34)$$

in the ordered phase. Simply evaluating  $S_o^{-1}$  from Eq. (28) at  $\tau = \tau_{\text{eq}}(\rho)$  yields a different law

$$S_o^{\text{thread}}(\rho; \tau_{\text{eq}}(\rho)) = \frac{1}{3}. \quad (35)$$

The difference in the ensembles is striking. Allowing  $\tau$  to vary in equilibrium promotes overall fluctuations in  $\rho$ .

## V. THERMODYNAMIC TRANSITION

We now turn to the determination of the full  $(\rho', d)$  phase plane of the athermal cutoff thread model. Given  $\tau_{\text{eq}}(\rho')$  defined by Eq. (19), we calculate equilibrium thermodynamics, now restricted simply to the isothermal, constant volume ensemble. One has

$$P_{\text{eq}} = \rho^2 \frac{\partial F_{\text{tot}}}{\partial \rho} + \rho^2 \frac{\partial F_{\text{tot}}}{\partial \tau} \frac{d\tau_{\text{eq}}}{d\rho} = \rho^2 \frac{\partial F_{\text{tot}}}{\partial \rho}, \quad (36)$$

using Eq. (19). The thermodynamic pressure is equal to the *constant- $\tau$*  pressure evaluated at  $\tau = \tau_{\text{eq}}(\rho')$ . While  $P_{\text{eq}}(\rho')$  and  $P(\rho', \tau)$  above are very different objects, (one is a function of  $\rho'$  alone, and the second is a function of both  $\tau$  and  $\rho'$ ), their numerical values are closely related.

The stability requirement on  $P_{\text{eq}}(\rho')$  is simply that  $\partial P_{\text{eq}} / \partial \rho' > 0$ . Figure 2 shows the generic behavior of  $P_{\text{eq}}$  in

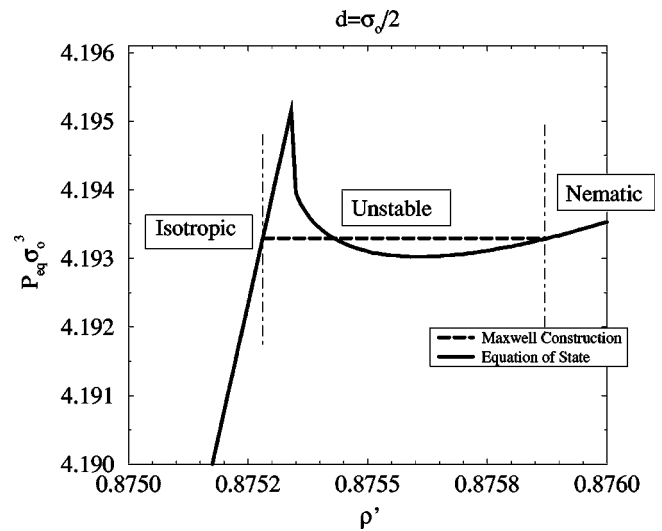


FIG. 2. Maxwell construction. The region between  $\rho'_N$  and  $\rho'_I$  (vertical dashed lines) is shown in detail for  $d = \sigma_o/2$ . The Maxwell construction, shown as a dashed line, ensures that  $F_{\text{eq}}(\rho')$  has the correct concavity globally.

the vicinity of the I–N transition for the case of  $d = \sigma_o/2$ .  $\rho' = 0.8753$  is the location of the “bare transition,” that is, this is the density at which  $\tau > 0$  first becomes lower in free energy than the isotropic phase. On the isotropic side, the pressure increases monotonically with  $\rho'$ . At the transition, the pressure drops suddenly, and then continues to drop before it reaches a local minimum and starts to increase again. Here, the fluid is linearly unstable to variations in  $\rho'$ . We must surround this unphysical region (containing the bare transition) via the equal areas construction of Maxwell. Let  $\rho'_I$  and  $\rho'_N$  be the values of  $\rho'$  which limit the biphasic window below and above, respectively. These densities are determined in the standard manner, requiring mechanical and thermodynamic equilibrium between the fluids held at  $\rho' = \rho'_I$  and  $\rho' = \rho'_N$  through a Maxwell equal-areas construction, as shown for  $d = \sigma_o/2$  case in Fig. 2. The solid dashed line indicates the pressure in the coexistence window, and true stability occurs only when  $\rho' > \rho'_N$  for the nematic phase, and for  $\rho' < \rho'_I$  in the isotropic phase. As required, in this region, the pressure is a monotonically increasing function of  $\rho'$ , and the characteristic coexistence of a first-order phase transition is apparent.

This type of analysis allows us to map out the entire  $\rho' - d$  phase plane of athermal, flexible polymers, as shown in Fig. 3. For very small  $d$ , the transition occurs at very small  $\rho'$ . Indeed, in the thread limit, we have

$$\rho'_I = \rho'_N = \frac{3d}{\sigma_o} \rightarrow \rho_c = \frac{18}{\pi\sigma_o^3}. \quad (37)$$

In this limit, the width of the coexistence region vanishes (inset to Fig. 4)), indicating the *continuous* nature of the thread transition. As  $d$  grows to finite values, the coexistence region widens, but is still extremely narrow, rising to just 0.2% of the isotropic phase boundary,  $\rho'_I$ . Thus,  $\rho'_I(d)$  and  $\rho'_N(d)$  appear to coincide in Fig. 3. The dashed line indicates the previously obtained *string* model result<sup>7,19</sup> (equivalently,

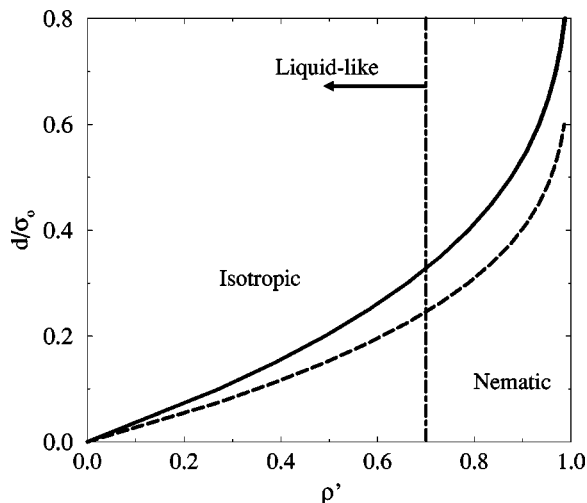


FIG. 3. Cutoff thread phase diagram ( $b=1$ ), defined by the phase boundary between I and N phases (solid line). The biphasic window is not resolved at this scale. The vertical dot-dashed line represents a liquidlike melt density. The dashed line shows the coexistence boundary for the athermal string model.

the choice of the cutoff thread model parameter,  $b=4/3$ . The latter is surprisingly close to the thread model prediction based on  $b=1$  in Eq. (5). This provides additional support for the physical sensibility of our construction of the thread with cutoff model.

If the I–N transition were not preempted by other physics (crystallization or vitrification), this model predicts a nematic phase for every flexible polymer species. Given  $\sigma_o$  and  $d$ , we can raise the system density to a physical value ( $\rho' < 1$ ) and force the transition. That nematic phases are apparently never (or very rarely) observed for  $d \approx \sigma_o$  polymers is understandable from Fig. 3. If we limit the transition density to liquid like values (say,  $\rho' = 0.7$ , or 70% of the isotropic close-packed density, as shown by the vertical dot-dashed line in Fig. 3), then the polymer segments must have

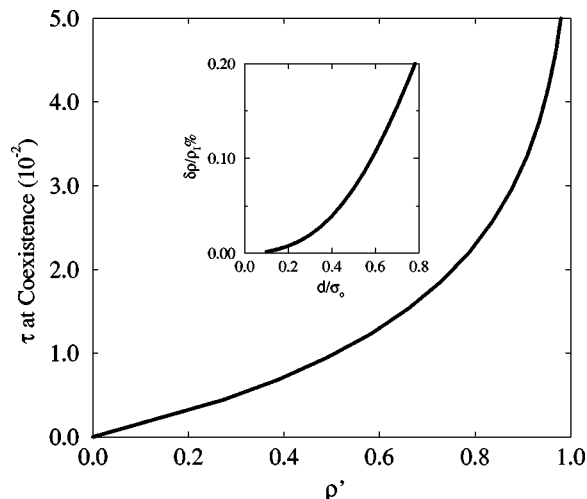


FIG. 4. Nematic order at coexistence,  $\tau_{\text{eq}}(\rho' = \rho'_N)$ , is shown as a function of  $\rho'_N$ . The ordering just at the transition is thus exceedingly weak, with  $\tau_{\text{eq}} = 2\%$  when  $\rho'_N$  is held at the melt-like value of 0.7. Inset is the biphasic width of the transition,  $(\rho_N - \rho_I)/\rho_I$ .

an aspect ratio  $\sigma_o/d$  exceeding  $\approx 3$ . This fits rather nicely with the known aspect ratios of thermotropic liquid crystalline polymers.<sup>1</sup> The string model result gives a more stringent (though still reasonable) condition that  $\sigma_o > 5d$ . Thus, as expected, the precise “minimum aspect ratio” required for nematic phases to exist is sensitive to the quantitative details of the statistical mechanical approximations and chain model.

A final property to note is that the transition for nonzero  $d$  is always first-order, and always towards a nematic phase. In the thread model, it appeared that both the nematic and discotic solutions existed in equilibrium. Allowing  $d > 0$  breaks the vital symmetry connecting the nematic and discotic configurations. The fact that the dislike  $\tau < 0$  branch of solutions is (apparently) not observed experimentally is consistent with our model predictions.

The weakness of the cutoff model transition is striking. In Fig. 4, we show the value of the order parameter just at the nematic limit of the coexistence window [that is,  $\tau_{\text{eq}}(\rho'_N(d))$  vs  $\rho'_N(d)$ ]. In keeping with the thread transition, the jump in the order parameter vanishes at  $d=0$  (continuous transition), and grows for any finite  $d$ . At a typical liquid density  $\rho' = 0.7$ , the jump in  $\tau_{\text{eq}}$  is only on the order of 2% of full alignment. This may be contrasted with the strong ( $\approx 60\%$ ) jump in the nematic order parameter for long-rigid, thin, rods,<sup>3</sup> and main chain thermotropics ( $\approx 20\% - 30\%$ ).<sup>8</sup>

Figure 5 shows on a larger scale the behavior of the equation of state for  $\sigma_o/d = 2, 4, \dots, 10$ . The thermodynamic width of the transition is too narrow to resolve in this plot. The appropriate scaled pressure is  $P_{\text{eq}}d^3$ , which, in the isotropic phase, has all dependence on  $d/\sigma_o$  encoded in the scale of  $\rho'$ . Thus, the five curves shown all provide the same pressure-density relationship in the isotropic phase. The isotropic-phase pressure grows toward a logarithmic divergence at  $\rho' = 1$ . Before this can happen, however, at the  $d$ -dependent transition density,  $\rho'_I < \rho' < \rho'_N$ , the pressure begins a much more gradual increase, approximately linearly. Given the scaling of the ordinate, it is clear that

$$P_{\text{eq}}d^3 \approx \rho' \frac{d^2}{\sigma_o^2}, \quad (38)$$

in the ordered phase. Thus, in keeping with the thread model predictions, the equilibrium pressure is nearly linear in the ordered phases. Such nearly linear behavior appears in simulations of needlelike molecules up to quite high packing fractions, and in simulations of hard, thin platelets.<sup>1,20</sup> The evolution of the nematic order is also shown in Fig. 5 by the dashed lines, which mark the iso- $\tau_{\text{eq}}$  lines of  $\tau = 0.1, \dots, 0.9$ , as  $\tau_{\text{eq}}$  evolves with increasing  $\rho'$ .

We determine the equilibrium dimensionless compressibility through numerically differentiating the equation of state, and one must take into account that  $d\tau_{\text{eq}}/d\rho' \neq 0$ . The symbol  $(\rho\kappa) \equiv (dP[\rho', \tau_{\text{eq}}(\rho')]/d\rho')^{-1}$  is the dimensionless, equilibrium compressibility of the chains with  $\tau$  free to vary, maintaining thermal equilibrium. This quantity, scaled by  $\sigma_o^2/d^2$ , collapses onto a master relation in the isotropic phase, as may be seen in the inset to Fig. 5. For  $d/\sigma_o$

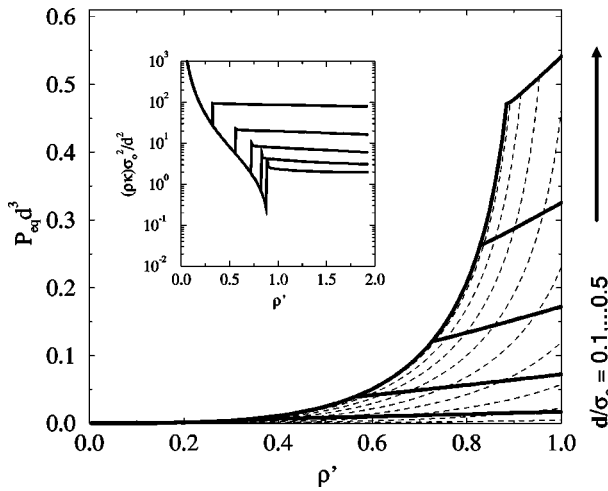


FIG. 5. The scaled pressure,  $P_{eq}d^3$ , is plotted, for  $d/\sigma_o=0.1, \dots, 0.5$  (solid curves, from bottom to top) and the iso- $\tau_{eq}$  lines for  $\tau=0.1, \dots, 0.9$  (dashed curves).  $\tau$  increases as  $P_{eq}$  decreases, or as  $\rho'$  increases. Inset is the dimensionless isothermal compressibility, which increases at the transition to a nearly constant value, again for  $d=0.1, \dots, 0.5$  from top to bottom.

$=0.1, \dots, 0.5$ ,  $(\rho\kappa)\sigma_o^2/d^2$  falls on a universal curve in the isotropic phase

$$(\rho\kappa) \frac{\sigma_o^2}{d^2} = \frac{3(1-\rho')}{4(\rho')^2}. \quad (39)$$

After the transition, the compressibility jumps dramatically to a (nearly) density independent value. Thus, the system's bulk thermodynamics become more liquidlike in the ordered phases.

Finally, we show in Fig. 6 the evolution of the absolute value of equilibrium nematic order parameter [Fig. 6(A)], as well as the evolution of the metastable discotic branch of solutions, [Fig. 6(B)], for  $d/\sigma_o=0.1, \dots, 0.5$ . At this level of detail, the jump in the order parameter at the transition is not detectable. However, the order parameter always grows rapidly for  $\rho' > \rho'_{IN}$ , and the approach to full discotic order seems to be more rapid than that of the true equilibrium nematic ordering. In the representation of Fig. 6, the orientational order ‘‘turns on’’ more rapidly as the aspect ratio increases in the sense that a scaled plot (not shown) of  $\tau_{eq}$  versus  $\rho'/\rho'_{IN}$  is more and more ‘‘step function’’ like as  $d \rightarrow 0$ . Very close to  $\rho'_{IN}$ ,  $\tau_{eq}$  increases in a mean field square root manner, (apart from its discontinuity) as analytically shown previously in the thread model limit.<sup>7</sup>

### VI. FLUID STRUCTURE

Structural information about the nematic fluid is easily calculated. As in Eqs. (2)–(4),  $\xi_z$  is the distance below which collective density fluctuations *along the  $\hat{z}$  axis* are correlated, and  $\xi_{\perp}$  is the correlation length for fluctuations lateral to  $\hat{z}$ . In Fig. 7(A) we show  $\xi_z$  as the I–N phase boundary is crossed. When scaled by  $d$  and plotted as a function of  $\rho'$ ,  $\xi_z$  collapses for all  $\sigma_o/d$ , *in the isotropic phase*

$$\xi_z(\tau_{eq}=0) = \frac{3d\sqrt{1-\rho'}}{2\rho'}. \quad (40)$$

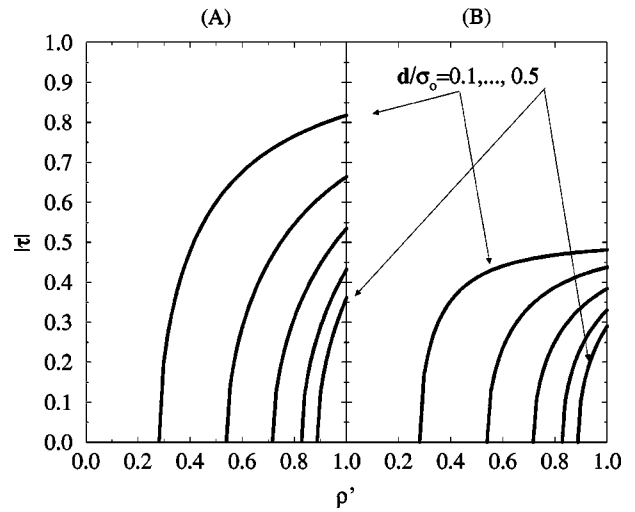


FIG. 6. Order parameter for nematic and discotic phases. (A) Nematic phase order parameter as a function of  $\rho'$  for  $d/\sigma_o=0.1, \dots, 0.5$ . All curves approach  $\tau=1$  for  $\rho' \gg 1$ . (B) The absolute value of the metastable discotic phase order parameter is plotted for the same values of  $d/\sigma_o$ . All curves approach  $|\tau|=1/2$  for  $\rho' \gg 1$ .

That is,  $\xi_z(\tau=0)$  diverges as  $\rho' \rightarrow 0$  (semidilute limit, for  $N \rightarrow \infty$ ), and vanishes at the incompressible limit,  $\rho' = 1$ . The first-order transition to the nematic phase occurs at a  $d/\sigma_o$  dependent density, so  $\xi_z$  no longer collapses onto a single scaling function for different aspect ratios. At the transition, there is a discontinuous jump in  $\xi_z$ , not observable on the scale of Fig. 7. However, it is clear that  $\xi_z$  becomes steadily larger up to the close-packed (isotropic) state, indicating that fluctuations of site density are longer ranged along the director than in the analogous isotropic fluid. So, while  $\kappa_T$  increases at the transition, indicating that the fluid becomes less ‘‘stiff,’’ this weakening takes place along the  $\hat{z}$  axis. At significantly large  $\rho' > 1$ ,  $\xi_z$  does decrease with increasing

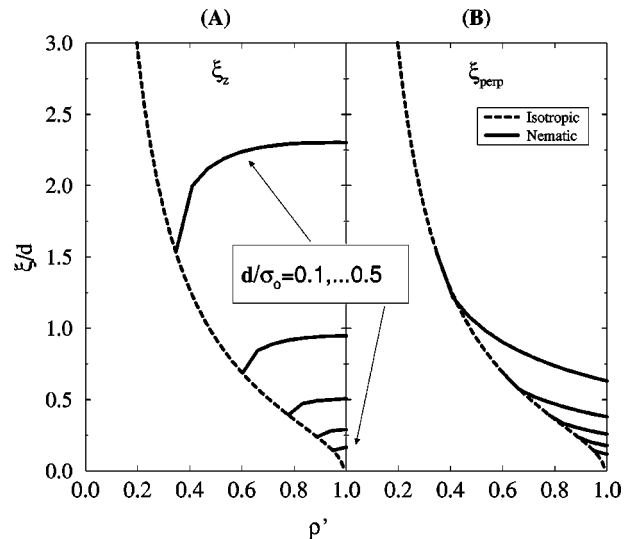


FIG. 7. Anisotropic screening lengths:  $\xi_z$  and  $\xi_{\perp}$  vs  $\rho'$ . (A) Parallel screening length,  $\xi_z(\rho', \tau_{eq})$ , for  $d/\sigma_o=0.1, \dots, 0.5$ , rises dramatically at the transition. The nonmonotonic response in  $\xi_z$  is increased as  $d \rightarrow 0$ . The dashed line is the isotropic-phase screening length, vanishing at  $\rho'=1$ . (B) Perpendicular screening length,  $\xi_{\perp}$ , for  $d/\sigma_o=0.1, \dots, 0.5$ .

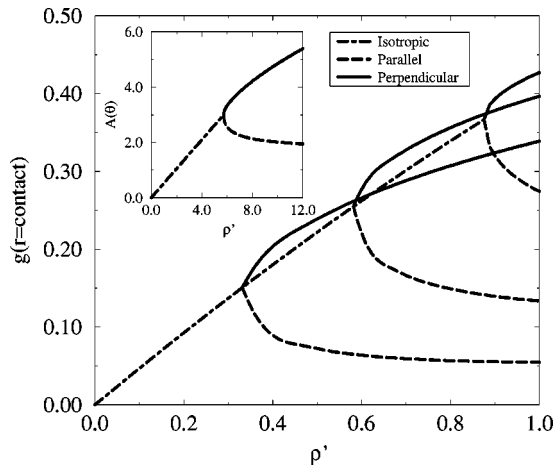


FIG. 8. Anisotropic  $g(\mathbf{r})$  at contact parallel (dashed curves) and perpendicular (solid curves) for  $d/\sigma_o = 1/8, 1/4, 1/2$ . The dot-dashed curve shows the behavior of the contact value in the isotropic phase. Inset is the analogous prediction of the thread model (Ref. 7).

density (not shown). In Fig. 7(B), we see that the lateral, or perpendicular, screening length  $\xi_{\perp}$  shrinks as  $\rho'$  increases into the ordered phase, although at much slower rate than the corresponding (extrapolated) isotropic phase. The liquid looks more concentrated laterally, although  $\xi_{\perp}$  does not literally vanish at the “close packed limit,”  $\rho' = 1$ . Comparing Figs. 7(A) and 7(B), it is obvious that density fluctuations can propagate more easily along the director than lateral to it in the ordered phases.

We determine  $g(\mathbf{r})$  numerically in the ordered phases. Particularly relevant to the *dynamics* of these liquid crystalline polymers is the *contact value* of the pair correlation function, which is the key quantity controlling the binary interchain “collision rate” between monomers.<sup>13,21</sup> In an isotropic fluid, increasing  $\rho$  always increases the contact value of  $g(\mathbf{r})$ , but in lyotropic liquid crystals, increasing the density enhances the orientational order and anisotropy which can introduce subtle competing effects.

In the liquid crystalline phases, the number of site-contacts changes continuously on the “contact sphere,”  $g(|\mathbf{r}|=d)$ . In particular, we show in Fig. 8 the behavior of the contact value of  $g(\mathbf{r})$  along and perpendicular to the nematic director, for  $d/\sigma_o = 1/8, 1/4, 1/2$ . Below the I–N transition,  $g(\mathbf{r})$  is isotropic. In the nematic phase, the number of contacts becomes much larger in the perpendicular direction than in the parallel direction. Thus, aligning the chains along the  $\hat{z}$  direction is expected to reduce (enhance) local friction parallel (perpendicular) to the director, relative to the isotropic behavior. For highly ordered nematics, the parallel contact value appears to saturate at a nonzero value which is a decreasing function of aspect ratio. The perpendicular analog becomes more slowly increasing with density and smaller (for strong alignment) than its isotropic fluid analog. Similar results for the (metastable) discoticlike phase are also easily obtained, but not shown here.

The behavior of the contact value in the cutoff model compares very well with that predicted by the thread model, as shown in the inset to Fig. 8. Of course, the definition of the contact value is somewhat ambiguous in the thread

model, since we take  $g(r=0) \equiv 0$ .<sup>7,12</sup> Trivially, the thread model contact value vanishes. However, one can ask how the quantity

$$A(\theta) = \left. \frac{\partial g(\mathbf{r})}{\partial r_{\theta}} \right|_{r=0}, \quad (41)$$

behaves, where  $r_{\theta}$  is the distance away from the origin along the azimuthal angle,  $\theta$ . Thus,  $A(\theta)$  is the *contact directional derivative*, describing the rate at which pair correlations increase in different directions. The thread case fairly well describes the detailed numerical results of the  $d \neq 0$  cutoff model. Results for the discoticlike phase are given elsewhere.<sup>7</sup>

We can make a further comparison to the prediction of the contact value for the related string model.<sup>7,19</sup> When  $\rho'$  grows beyond the transition value,  $g(\mathbf{r})$  becomes markedly *negative* along the longitudinal direction. The average nature of the string closure ensures that  $g(r) > 0$  for  $r > d$  (the physically interesting domain) in the isotropic phase, but the condition that  $\int_0^d d^3 r g(r) = 0$  is not strong enough in the anisotropic phase to ensure the positivity of  $g$  for  $r > d$ . Thus, we find with increasing  $\tau$  that  $g(\mathbf{r})$  becomes more and more negative along the nematic director, clearly a disturbing result. This is our main motivation for employing the cutoff thread model in practice.

In Fig. 9, we display the ordered-phase behavior of the cohesive energy,  $U_{\text{coh}}$ , as defined in Paper I, through the I–N transition

$$U_{\text{coh}} = \rho \int d\mathbf{r} g(\mathbf{r}) v(\mathbf{r}), \quad v(\mathbf{r}) = -\frac{v_o e^{-r/a}}{r/a}. \quad (42)$$

In the mean field limit [in which  $g(\mathbf{r}) = 1$  in Eq. (42)],  $U_{\text{coh}} = -4\pi a^3 \rho v_o$ . Therefore, the “differential cohesion,”

$$B_{\text{coh}}(\rho') \equiv \frac{U_{\text{coh}}(\rho', \tau)}{U_{\text{coh}}(\rho' = 1, \tau = 0)} - \rho', \quad (43)$$

is a measure of the nonmean field nature of  $U_{\text{coh}}$ .  $B_{\text{coh}}(\rho')$  vanishes exactly in the mean field limit, and it may also be used to gauge the relative cohesion of the nematic, isotropic, and discotic phases. We show this quantity for various values of the range of the interaction,  $a/d = 1/5, 1, 5$  in Fig. 9. Clearly, when  $a \gg d$ , the cohesion becomes more mean field-like. For  $d = \sigma_o/2$  and  $d = \sigma_o/8$ , the cohesion in the nematic phase is shown as the solid line. Clearly, the nematic phase is *less cohesive* than the isotropic phase (the upper solid curves in each panel). Interestingly, the metastable *discotic* solution has a cohesion in between that of the isotropic and nematic phases, and we shall discuss the implications of this below.

## VII. RIGID RODS

An important benchmark for the current theory can be found in Onsager’s original description of liquid crystallinity in long, thin rods.<sup>13</sup> The Onsager solution is exact as the rods become thinner relative to their length  $L$ , i.e.,  $L/d \gg 1$ , where  $d$  is the rod thickness. We may anticipate that the Onsager problem is the extreme case of a flexible polymer whose statistical segment length grows to the end-to-end

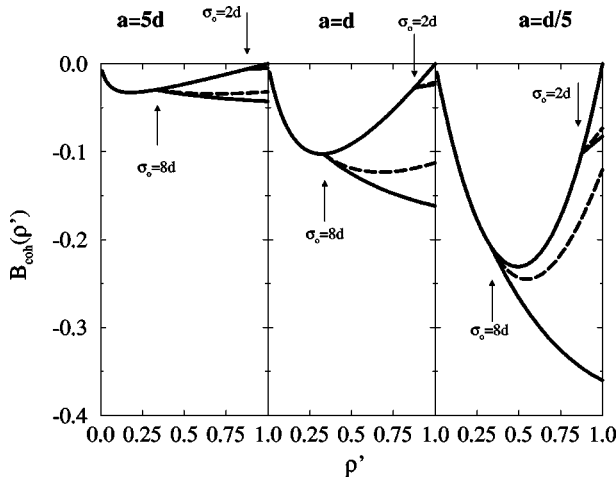


FIG. 9. Differential cohesion,  $B_{\text{coh}}$ , defined in Eq. (43) for  $a/d=5, 1, 1/5$ , and  $d/\sigma_o=1/8, 1/2$ .  $B_{\text{coh}}$  in the isotropic phase (upper solid curve) gets smaller and smaller as  $a/d$  grows, indicating that the cohesion becomes mean fieldlike for large  $a$ . The arrows indicate  $\rho'_{\text{N}}$  at both of the considered aspect ratios. The lower solid lines show  $B_{\text{coh}}$  in the nematic phase, and the dashed lines show the discotic-phase cohesion.

length of the polymer. Thus, the cutoff-thread and the Onsager description bracket the response of semiflexible polymers.

We adopt the following single-chain scattering function<sup>22</sup>

$$\omega_{\text{rod}}(\mathbf{q}) = \frac{L/d}{\sqrt{1 + (L^2/18)((1+2\tau)q_z^2 + (1-\tau)q_{\perp}^2)}}. \quad (44)$$

This is appropriate for one-dimensional mass fractals<sup>22</sup> with a radius of gyration:  $R_g^2 = L^2/12$ . For isotropic rods, this function exactly captures the  $qR_g \ll 1$  regime, and the intermediate scaling regime power law,  $\omega_{\text{rod}}(\mathbf{q}) \approx (qd)^{-1}$ . This is a simple, but crude, model of ‘‘Gaussian rigid rods’’ whose overall nematic ordering is given by  $\tau$ . Here, the ‘‘degree of polymerization’’ of the rod,  $N$ , is related to the length of the rod,  $L$ , and its thickness,  $d$ , via  $L = Nd$ . Thus, Eq. (44) should be viewed as a continuum level approximation to the structure factor of a rigid rod composed of  $N$  tangent interaction sites of diameter  $d$ .

Again we can define the total site–site correlation function

$$h(\mathbf{q}) = \frac{c_o \omega_{\text{rod}}^2(\mathbf{q})}{1 - \rho c_o \omega_{\text{rod}}(\mathbf{q})}, \quad (45)$$

where again we have taken  $C(\mathbf{q}) = c_o$  when  $q < \pi b/d$ , and vanishes otherwise. Here,  $\rho$  is not the number density of rods, but rather the site number density:  $\rho = N\rho_{\text{rod}} = L\rho_{\text{rod}}/d$ . We anticipate that for the  $L \gg d$  case of present interest the liquid crystalline transition for these rods occurs at vanishingly small  $\rho$ , and so we adopt the *infinite dilution* limit in describing  $h(\mathbf{q})$

$$\begin{aligned} h(\mathbf{q}) &\approx c_o \omega_{\text{rod}}^2(\mathbf{q}) \\ &= \frac{c_o L^2/d^2}{1 + [(1+2\tau)L^2 q_z^2/18] + [(1-\tau)L^2 q_{\perp}^2/18]} \end{aligned} \quad (46)$$

$$\approx \frac{18c_o}{q^2 d^2 (1 - \tau + 3\tau^3 u_{\theta}^2)} + O[d/L]. \quad (47)$$

The core constraint  $h(\mathbf{r}=0) = -1$  is directly enforced, thereby determining the direct correlation parameter,  $c_o$

$$-1 = \int_0^{\pi b/d} \frac{q^2 dq}{(2\pi)^2} \int_{-1}^1 du_{\theta} h(\mathbf{q}), \quad (48)$$

where we note that the upper cutoff in wave-vector space is *essential* for the integral in Eq. (48) to converge.<sup>22</sup> Thus, there does not exist a universal thread limit for rods; their thickness,  $d$ , is *always* a relevant length scale. Eqs. (46)–(48) yield

$$c_o^{\text{rod}} = -d^3 \frac{\pi \sqrt{\tau(1-\tau)}}{3\sqrt{3}b \tan^{-1} \sqrt{3\tau/(1-\tau)}}. \quad (49)$$

Notice that  $c_o^{\text{rod}}$  is *independent* of density, implying that the compressibility is constant, the pressure scales as  $\rho^2$ , and the excess free energy associated with the excluded volume interactions is  $\sim \rho$ . In particular, we have

$$S_o^{\text{rod}} = \frac{1}{\rho |c_o(\tau)|}, \quad (50)$$

$$P^{\text{rod}} = \frac{1}{2} \rho^2 |c_o(\tau)|, \quad (51)$$

$$F_{\text{site}}^{\text{rod}} = \frac{1}{2} \rho |c_o(\tau)|. \quad (52)$$

Thus, the infinite dilution PRISM theory is equivalent to a second-virial level description of the many body thermodynamics, as is indeed appropriate for the Onsager analysis.

A crude estimate of the entropy associated with holding a rod in the anisotropic orientation of a given  $\tau$  is the same as we used for the Gaussian polymers, except the orientation of each ‘‘site’’ is determined by the rigidity of the entire object. That is,

$$F_{\text{ideal}}^{\text{rod}} = -\frac{d}{L} \log[(1-\tau)\sqrt{1+2\tau}]. \quad (53)$$

Thus, the orientational entropy per site is simply the orientational entropy of the entire rod, divided by  $N$ . Rods will much more readily form liquid crystalline phases than flexible polymers. While  $F_{\text{site}}$  can be comparable to its value in the flexible polymer case,  $F_{\text{ideal}}$  is smaller by a factor of molecular weight, and it is  $F_{\text{ideal}}$  that stabilizes the isotropic phase.

The small order parameter expansion of the total free energy is given by

$$F_{\text{tot}}^{\text{rod}} = F_{\text{site}}^{\text{rod}} + F_{\text{ideal}}^{\text{rod}} = F_0 + F_2 \tau^2 + F_3 \tau^3, \quad (54)$$

where

$$F_2 = \frac{3d}{2L} - \frac{2\pi d^3 \rho}{45b}. \quad (55)$$

$F_2$  changes sign (and hence, the isotropic phase becomes linearly unstable to orientational fluctuations) when

$$\rho = \rho_c \equiv \frac{135b}{4\pi d^2 L}. \quad (56)$$

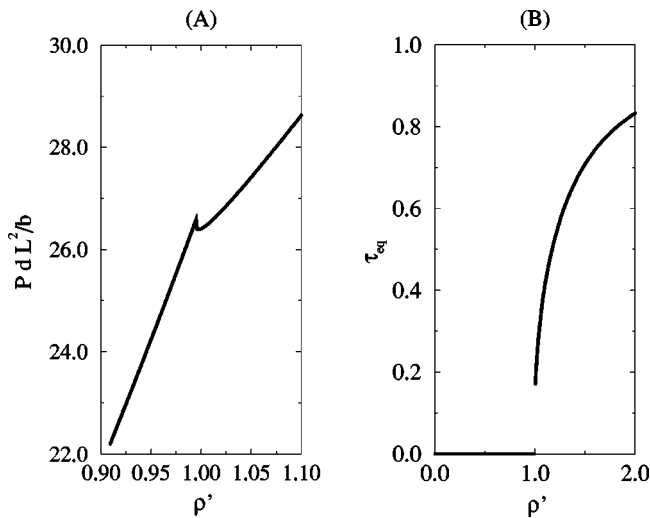


FIG. 10. PRISM prediction for long, thin rods. (A) Equation of state. The scaled pressure is nonmonotonic in the vicinity of  $\rho' = 1$ , and requires a Maxwell construction. (B) Order parameter. The nematic order jumps to  $\approx 20\%$  at the transition, and increases steadily.

So, when the rod density,  $\rho_{\text{rod}} = d\rho/L \approx d^{-1}L^{-2}$ , the isotropic phase becomes unstable. This relation agrees with the scaling form of the transition density in the Onsager theory. The nematic transition occurs at an exceedingly small volume fraction of rods:  $\phi_c \sim d/L$ . We take  $\rho \equiv \rho' \rho_c$ , so this instability occurs at a scaled density of  $\rho' = 1$ .

We now analyze  $F_{\text{tot}}^{\text{rod}}$ , and look for the thermodynamic instability of the system. Numerically, it is easy to verify that the transition is first-order, and toward the nematic phase

$$NF_{\text{tot}} = \frac{15}{8} - \frac{1}{7}\tau^3 + \frac{123}{140}\tau^4 + \dots, \quad (57)$$

when  $\rho' = 1$ . The strongly negative coefficient of the  $\tau^3$  term, and the stabilizing value for the  $\tau^4$  coefficient, ensures a relatively strong transition to a nonzero  $\tau > 0$ .

A Maxwell equal area construction is required by the form of the equation of state in Fig. 10(A), since the pressure is markedly nonmonotonic in the vicinity of  $\rho' = 1$ . The width of the predicted biphasic window is on the order of 1% of the transition density, much narrower than that predicted by Onsager theory ( $\approx 30\%$  width).<sup>3</sup> The Onsager result for the rod density at which the nematic first appears is  $\rho \approx 4.2/(d^2L)$ , roughly a factor of 2.5 smaller than our prediction in Eq. (56), based on the choice of  $b = 1$  for the cutoff parameter. This modest quantitative difference can be removed entirely by choosing  $b \approx 0.4$ , that is, by adjusting the cutoff wavevector. The dimensionless osmotic compressibility is nearly constant in the nematic phase and is roughly a factor of 2 larger than in the isotropic fluid. As shown in Fig. 10(B), the order parameter jump at the nematic edge of the coexistence window is  $\tau_{\text{eq}} \approx 0.2$ , again weaker than that predicted by Onsager theory ( $\approx 70\%$ ). The manner in which the order parameter rises is, however, consistent with the exact solution. The weaker nature of our first-order transition compared to Onsager theory is hardly surprising given our crude treatment of nonzero monomer volume, oversimplified  $\omega_{\text{rod}}(\mathbf{q})$  in Eq. (44), and single-rod entropy in Eq. (53).

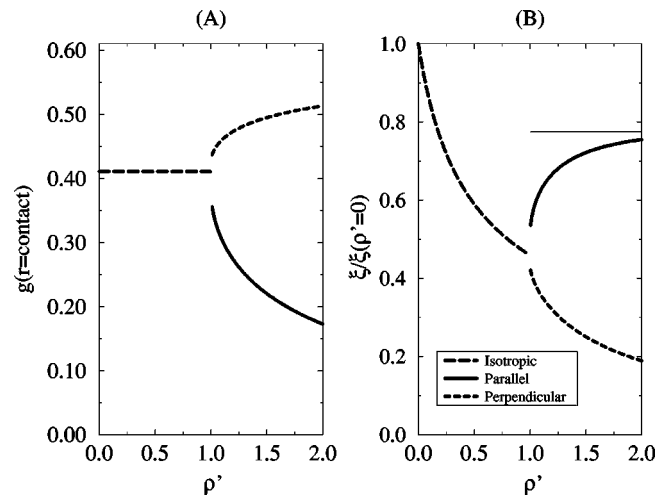


FIG. 11. Structural quantities for rods. (A) Contact value of  $g(\mathbf{r})$ . As in the flexible polymer case, the contact value of the pair correlation increases perpendicular to the order, and decreases along the order. (B) Screening lengths  $\xi_z$  (solid curve) and  $\xi_{\perp}$  scaled by their zero-density values are plotted. As in the flexible polymer case, fluctuations are greater along the director than lateral to it. The asymptotic limit of  $\xi_z$  is shown as the thin horizontal line.

The theory prediction for the contact value of the pair correlation function is an easily calculated quantity, at least numerically, and is shown in Fig. 11(A). This second virial theory for the structure of the nematic rod fluid has a  $c_o(\tau)$  which has no explicit dependence on  $\rho'$ . Therefore,  $g(\mathbf{r})$  has no explicit dependence on density, so that  $g(|\mathbf{r}| = d)$  is a constant in the isotropic phase. When the nematic transition occurs,  $c_o(\tau_{\text{eq}}(\rho'))$  gains an implicit dependence on  $\rho'$ , and we see the same characteristic features found for flexible polymers. The contact value is, of course, discontinuous. It grows perpendicular to the director (so that the collision rate in the fluid becomes enhanced in the lateral direction) and decreases along the director (so that rods may move more freely along the director).

In Fig. 11(B), we show the rod theory values for  $\xi_z$  and  $\xi_{\perp}$ , scaled by their maximal (low density) values in the isotropic phase. Below the transition,  $\xi_z = \xi_{\perp}$ , but above the transition,  $\xi_z$  grows while  $\xi_{\perp}$  falls. Asymptotically

$$\frac{\xi_z}{\xi(\rho' = 0; \tau = 0)} \approx \sqrt{\frac{3}{5}} - \frac{32}{75\sqrt{15}\rho'}, \quad (58)$$

$$\frac{\xi_{\perp}}{\xi(\rho' = 0; \tau = 0)} \approx \frac{8\pi}{15\sqrt{15}\rho'}, \quad (59)$$

as  $\rho' \rightarrow \infty$ . Hence,  $\xi_z$  rises to  $\sim 80\%$  its dilute isotropic value, while  $\xi_{\perp}$  vanishes altogether, far into the ordered phase.

Thus, with very little calculational effort, our anisotropic version of PRISM theory correctly reproduces the scaling form of the transition density, and all other qualitative features found in the benchmark Onsager theory of the I-N transition of rigid rods. Our simplified treatment rests on two approximate relations which may be systematically improved. First, the choice for  $\omega_{\text{rod}}$  is, although qualitatively reasonable, clearly motivated heuristically. Nonetheless, the

prediction for  $S(\mathbf{k}=0)$  in the isotropic phase essentially reproduces that of a full numerical PRISM-PY calculation on tangent-bead rigid rods.<sup>23</sup> The “exact” single chain scattering of a rod may be calculated numerically, given a prescription for  $f(\Omega)$ , the orientational distribution function for the rods. That is,  $\omega_{\text{rod}}[f]$  is a functional of  $f(\Omega)$ , just as the second virial coefficient in the Onsager theory is a functional of  $f(\Omega)$ . Secondly, the ideal orientational entropy,  $F_{\text{ideal}}$  is not likely to be of such a simple form as we have used here, but is also a functional of  $f(\Omega)$

$$F_{\text{ideal}} = \int \frac{d\Omega}{4\pi} f(\Omega) \log f(\Omega). \quad (60)$$

Thus, one could use the PRISM formalism to construct an approximate (though more realistic)  $F_{\text{site}}[f]$ , plus the exact  $F_{\text{ideal}}[f]$ , and minimize the total free energy with respect to the distribution  $f(\Omega)$ . This will allow the determination of the liquid crystallinity of not only long, thin rods, but finite thickness rods, bendable rods, and semiflexible polymers. Indeed, the theory may be applied to any object whose  $\omega$  one can deduce.

### VIII. DISCUSSION

One technical peculiarity surrounding the entire formalism is the scaling of  $\rho'$ . We have identified throughout  $\rho' = 1$  with the maximal density state in which monomers are so tightly squeezed together that they fill all available space. This literally incompressible state (incompressible in the sense that  $S_o = 0$  and that there is no more “empty” space that can be occupied by monomers) does *not* occur at a universal value of the traditional packing fraction variable,  $\eta \equiv \rho \pi d^3/6$ , but rather at a  $\sigma_o$  (or aspect ratio) dependent packing fraction:

$$\eta_{\text{max}} = \rho_{\text{max}}(\tau=0) \frac{\pi d^3}{6} = \frac{d^2}{\sigma_o^2}, \quad (61)$$

based on the choice  $b = 1$  in Eq. (5). Curiously, for “tangent bead” type flexible polymers (defined as  $\sigma_o = d$ )  $\eta_{\text{max}} = 1$ , which is exactly the incompressible state predicted by the PY theory of hard spheres.<sup>21</sup> In general, the close-packed isotropic state of polymers should depend on the chain aspect ratio, and intuitively, is expected to decrease with  $\sigma_o/d$  as predicted by Eq. (61). This type of scaling first appeared in studies of the string closure,<sup>9,19</sup> but its theoretical foundation is somewhat clouded by Fuch’s exact solution of the PRISM PY closure for the isotropic phase of  $\sigma_o \neq d \neq 0$  Gaussian chains which does not exhibit  $\rho'$  as the scaled density.<sup>16</sup>

Even more curious, is the fact that the maximal density in our model increases with  $\tau$ . That is, for a given alignment,  $\tau$ , there is always a logarithmic divergence in the pressure at  $\rho' = \rho'_{\text{max}}$ , given by Eq. (7) above. That fact that the maximum density increases with alignment is a physically sensible trend. However, we have adopted a conservative interpretation here: the close-packed density of the  $\tau = 0$  state is the maximal density under all conditions. This is done since the increase of  $\rho_{\text{max}}$  with  $\tau$  is surely greatly exaggerated by our simple cutoff-thread model, as dramatically illustrated by the fact that  $\rho_{\text{max}}(\tau) \rightarrow \infty$  as  $\tau \rightarrow 1$ . This uncontrolled growth

of  $\rho_{\text{max}}$  is also responsible for weakening the model predictions for the strength of the I–N transition. While monomers from other chains are (approximately) excluded from overlapping monomers on a test chain, the monomers on the test chain itself are modeled as belonging not to a *self-avoiding* anisotropic walk, but rather an arbitrarily interpenetrating walk. We suspect that handling the intrachain excluded volume self-consistently,<sup>15</sup> more accurately indexing the available nematic states (via a more numerically intensive, yet precise  $\omega(\mathbf{q})$ ), and rigorously enforcing the exclusion requirement that  $g(\mathbf{r}) \equiv 0, |\mathbf{r}| < d$  will largely solve this problem.

Although we have limited our interest to strictly athermal interactions, it is possible to estimate the effect of weak attractive forces on the anisotropic liquid crystalline phases studied here.<sup>9,19</sup> Inspired by the high temperature approximation (HTA), the repulsive excluded volume interactions are assumed to control the liquid structure in both the isotropic and liquid crystal phases. Attractions contribute an internal energy per site,  $U_{\text{coh}}$  of Eq. (42), to the free energy,  $F_{\text{tot}}$ . Its minimization with respect to  $\tau$  now implies that  $\tau_{\text{eq}}$  is a function of not only  $\rho'$  but also the range of the interaction and its strength,  $v_o$ . We have considered the magnitude of such a cohesive energy term in Paper I,<sup>10</sup> and generally the cohesion in the isotropic phase is superior to that in the liquid crystal phases. That is,  $|U_{\text{coh}}|$  is maximized for  $\tau = 0$ . Figure 9 shows that if we compare  $U_{\text{coh}}$  for the nematic (solid lines) and discotic (dashed lines), that the metastable discotic phase has more cohesion than the nematic, stable phase. That is, there is a hierarchy of cohesion,  $I > D > N$ , so that we may anticipate that adding  $U_{\text{coh}}$  at the level of  $F_{\text{tot}}$  can drive a sequence of *thermotropic* transitions, including an order–order transition from the nematic solution to the discotic as the temperature is lowered. We have investigated the phase behavior based on this so-called thermodynamic perturbation theory, and such transitions do in fact occur<sup>24</sup> when  $a \ll d$ . Moreover, we find that the very existence of a liquid phase (i.e., the simultaneous presence of both a critical point and a triple point) is a delicate issue depending on material specific quantities such as  $a/d$  and aspect ratio.<sup>24</sup> Thus, our anisotropic PRISM description of the I–N transition is capable of modeling not only lyotropic, but also thermotropic experiments, in a single unified formalism.

The fact that we have chosen an analytically tractable form for  $\omega(\mathbf{q})$  is not necessary. Liquid crystallinity in truly semiflexible chains can be addressed, with recourse to a fully numerical solution of the PRISM PY equations. Moreover, a semianalytic theory of semiflexible chains can be constructed by using a  $\omega(\mathbf{q})$  which smoothly interpolates between an ideal coil form for  $q\xi_p < 1$  and rigid-rod form for  $q\xi_p > 1$ , where  $\xi_p$  is the chain persistence length. Also, our treatment of the rod problem is not limited to  $L \gg d$ , but can sensibly account for finite size effects, and isotropic attractions. We find that attractions at the second virial (or infinite dilution) level quickly introduce unphysical instabilities which can only be handled correctly by abandoning the virial approximation, and investigating properties at finite rod volume fractions. Such a program is clearly feasible with our ap-

proach, and would allow treatment of liquid crystalline melts.

One word must be said regarding the role of the cutoff scale parameter,  $b$ . Clearly,  $b$  must be on the order of 1, but its precise value is not determined internally by the present thread-like model. As pointed out above, choosing  $b=4/3$  forces agreement between the string and cutoff thread models, at least as far as the density at which the isotropic phase becomes literally incompressible. Other choices for  $b$  are, of course, possible. The exact value of  $b$  has direct physical consequences. For example, the minimum  $d$  at which athermal liquid crystalline phases appear in Fig. 3 is on the order of  $d/b=\sigma_o/4$ . Choosing  $b=2$  or  $b=1/2$  could move this minimum  $d$  as high as  $\sigma_o/2$  (still reasonable), or as low as  $d=\sigma_o/8$ .

Finally, we note that our theory is of a *mean field* nature, in the sense that any spatial texture of the director field and fluctuations of the order parameter are ignored. We thus rule out topological defects in the ordered phases.<sup>2</sup> Treating these physically relevant effects requires a theory beyond our present liquid state approach.

## IX. CONCLUSIONS

We have applied an anisotropic version of PRISM theory<sup>10</sup> to the problem of liquid crystallinity in flexible polymers. Given a statistical segment length,  $\sigma_o$ , and a hard-core diameter,  $d$ , we demonstrate a first-order transition from an isotropic to a nematic phase as concentration is increased. Inducing this athermal transition requires  $\sigma_o \geq 4d$ , which is close to the observed minimum aspect ratios of existing thermotropic melt liquid crystal polymers. The transition is exceedingly weak, even for rigid-rod polymers, but systematic improvement of the theory is possible beyond the crude, yet analytically tractable, theory we present here.

In the nematic phase, we demonstrate the anisotropic screening of density fluctuations, and show that these fluctuations are farther ranged along the nematic director than lateral to it. Also, the contact value of the pair correlation function is significantly smaller along the director than lateral to it. Both of these results have the natural consequence that the chain self-diffusion is expected to be larger along the director than lateral to it.

The effect of adding attraction between monomer sites can be included in many approximate ways, thus allowing the study of the full temperature and density dependence of the liquid crystal phase diagram. An advantage of the PRISM framework is that the discussion is not limited to this ensemble, but results can be quickly recast so as to determine the more experimentally convenient *pressure* and *temperature* ensemble.<sup>24</sup> Combined with the innate ability of PRISM

to make *quantitative* predictions when given atomistically detailed single-chain information, this raises the realistic possibility that first-principles calculations of the thermodynamics, miscibility, and structure of liquid crystalline polymers may become possible.

## ACKNOWLEDGMENTS

This work was performed at the University of Illinois at Urbana Champaign and supported by the U.S. DOE Division of Materials Science Grant No. DEFG02-96 ER45539 through the University of Illinois Materials Research Laboratory. Helpful discussions with D. Chandler are gratefully acknowledged.

- <sup>1</sup>D. Frenkel, Les Houches, Session L1, 1989 *Liquids, Freezing, and Glass Transition*, edited by J. P. Hansen, D. Levesque, and J. Zinn-Justin, (Elsevier, B. V., 1991); G. J. Vroege and H. N. W. Lekkerkerker, Rep. Prog. Phys. **55**, 1241 (1992).
- <sup>2</sup>P. G. deGennes, *Physics of Liquid Crystals* (Oxford University Press, Oxford, 1974).
- <sup>3</sup>L. Onsager, Ann. (NY) Acad. Sci. **51**, 627 (1949).
- <sup>4</sup>P. G. deGennes, *Scaling Concepts in Polymer Physics* (Cornell University Press, Ithaca, 1979).
- <sup>5</sup>P. J. Flory, *Statistical Mechanics of Chain Molecules* (Interscience, New York, 1969).
- <sup>6</sup>M. Doi and S. F. Edwards, *The Theory of Polymer Dynamics* (Oxford Univ. Press, New York, 1986).
- <sup>7</sup>G. T. Pickett and K. S. Schweizer, J. Chem. Phys. **110**, 6597 (1999).
- <sup>8</sup>E. T. Samulski, Faraday Discuss. Chem. Soc. **79**, 7 (1985); I. A. Hussein and M. C. Williams, Macromol. Rapid Commun. **19**, 323 (1998).
- <sup>9</sup>For reviews, see K. S. Schweizer and J. G. Curro, Adv. Chem. Phys. **98**, 1 (1997); Adv. Polym. Sci. **116**, 319 (1994).
- <sup>10</sup>G. T. Pickett and K. S. Schweizer, J. Chem. Phys. **112**, 4869 (2000), preceding paper.
- <sup>11</sup>S. Sen, J. M. Cohen, J. D. McCoy, and J. G. Curro, J. Chem. Phys. **101**, 9010 (1994); S. Sen, J. D. McCoy, S. K. Nath, J. P. Donley, and J. G. Curro, *ibid.* **102**, 3431 (1995); B. Mulder, Phys. Rev. A **35**, 3095 (1987).
- <sup>12</sup>K. S. Schweizer and J. G. Curro, Macromolecules **21**, 3070, 3082 (1998); **21**, 3082 (1988); Chem. Phys. **149**, 105 (1990).
- <sup>13</sup>K. S. Schweizer, M. Fuchs, G. Szamel, M. Guenza, and H. Tang, Macromol. Theory Simul. **6**, 1037 (1997).
- <sup>14</sup>There is some scattering evidence that side-chain thermotropics maintain the constancy of their overall radius of gyration through the isotropic-nematic transition, and well inside the ordered phase. See, R. G. Kirste and H. G. Ohm, Makromol. Chem., Rapid Commun. **6**, 179 (1985).
- <sup>15</sup>J. Melenkevitz, J. G. Curro, and K. S. Schweizer, J. Chem. Phys. **99**, 5571 (1993); C. J. Grayce, A. Yethiraj, and K. S. Schweizer, *ibid.* **100**, 6857 (1994).
- <sup>16</sup>M. Fuchs, Z. Phys. B **103**, 521 (1997).
- <sup>17</sup>C. M. Marques and G. H. Fredrickson, J. Phys. II (France) **7**, 1805 (1997).
- <sup>18</sup>D. Chandler, Phys. Rev. E **48**, 2898 (1993).
- <sup>19</sup>A. P. Chatterjee and K. S. Schweizer, Macromolecules **31**, 2353 (1998).
- <sup>20</sup>R. Eppenga and D. Frenkel, Mol. Phys. **52**, 1303 (1984).
- <sup>21</sup>J. P. Hansen and I. R. McDonald, *Theory of Simple Liquids* (Academic, London, 1986).
- <sup>22</sup>M. Fuchs and K. S. Schweizer, J. Chem. Phys. **106**, 347 (1997).
- <sup>23</sup>A. P. Chatterjee and K. S. Schweizer (in preparation).
- <sup>24</sup>G. T. Pickett and K. S. Schweizer (in preparation).